Available online at www.sciencedirect.com
SCIENCE DIRECT®
Thermochimica Acta 420 (2004) 145–154
thermochimica acta
www.elsevier.com/locate/tca

Synthesis and characterization of V-MFI obtained in fluoride-containing medium

M. Veltri [a,*], P. De Luca [a], J. B.Nagy [b], A. Nastro [a]

[a] *Dipartimento di Pianificazione Territoriale, Università della Calabria, via Pietro Bucci, I-87036 Arcavacata di Rende CS, Italy*
[b] *Laboratoire de RMN, Facultés Universitaires N.D. de la Paix, B-5000 Namur, Belgium*

Received 30 July 2003; accepted 8 December 2003
Available online 8 July 2004

Abstract

Crystallization fields for the formation of V-MFI were determined from gels of composition: xNa$_2$O–yVO$_2$–7NaF–ySO$_3$–zSiO$_2$–2TPABr–260H$_2$O at 190 °C with $3.6 \leq x \leq 14.4$ and $2.1 \leq y \leq 7.1$ for $z = 12.0$ and with $0.3 \leq y \leq 4.2$ and $4.0 \leq z \leq 12.0$ for $x = 3.6$; TPA = tetrapropylammonium ions. The crystallization curves were analysed together with the various intermediate phases using XRD, pH of mother liquors, thermal analysis and SEM. The final samples were analysed, in addition, by multinuclear NMR. It is concluded, that V can be introduced into the MFI framework as V(IV) ions, accompanied by the presence of two SiOH defect groups per V atom introduced. The ^{51}V-NMR signal due to V(V) can only be detected when additional vanadium-containing siliceous phases are formed.

Keywords: V-MFI; Zeolite; Alkalinity; Crystallization; TPA$^+$ ions

1. Introduction

Isomorphous framework substitution in zeolites is a very important task, because that way both their acidic and redox properties can be modulated [1–3]. The vanadium silicate molecules sieves have been found to be active in ammoxidation of alkanes, epoxidation of alkanes and allylic alcohols, and oxidation of aromatic compounds [4–7]. The activity and selectivity of V-MFI are strongly dependent on the structure and location of V species, because that way their accessibility and coordination with absorbate molecules can be different.

The synthesis of V-MFI is made essentially using either trivalent or tetravalent vanadium sources [3]; for example, vanadyl sulfate [4,8–10] or vanadyl oxalate [11] have been successfully used to introduce vanadium in the MFI framework.

On the other hand, it was demonstrated that the fluoride-containing medium is the very efficient one to introduce various elements in tetrahedral framework positions [12]. This method has been successfully applied to introduce boron [13], iron [14], gallium [15] or cobalt [16] at least partially in the framework.

The present work is devoted to the synthesis of V-MFI zeolite at a high vanadium content. The final crystalline phases were analysed by XRD, chemical analysis, thermal analysis, SEM and multinuclear NMR.

2. Experimental

Gels of the following compositions were prepared: xNa$_2$O–yVO$_2$–7NaF–ySO$_3$–zSiO$_2$–2TPABr–260H$_2$O with tetrapropylammonium (TPA) and $3.6 \leq x \leq 14.4$ and $2.1 \leq y \leq 7.1$ for $z = 12$ and for $x = 3.6$, $0.3 \leq y \leq 4.2$ and $4.0 \leq z \leq 12.0$. Two clear solutions were first prepared, an alkaline one and an acidic one. The alkaline solution was prepared by mixing sodium silicate solution (8% Na$_2$O, 27% SiO$_2$, 65% H$_2$O; Merck) with sodium hydroxide (50 wt.% aqueous solution, Carlo Erba). The acidic solution was prepared adding NaF (Carlo Erba) to

* Corresponding author. Tel.: +39 0984 496 772; fax: +39 0984 496 787.
E-mail addresses: maria.veltri@unical.it (M. Veltri), p.deluca@unical.it (P. De Luca), janos.bnagy@fundp.ac.be (J. B.Nagy), a.nastro@unical.it (A. Nastro).

0040-6031/$ – see front matter © 2004 Elsevier B.V. All rights reserved.
doi:10.1016/j.tca.2003.12.034

distilled water, then after solubilizing the salt, $VOSO_4 \cdot 5H_2O$ (Riedel-de Haën) and TPABr (Fluka) were dissolved. The acidic solution was poured into the alkaline solution under continuous stirring in order to obtain an homogeneous gel. The pH of these gels was systematically measured. Parts of the gel were then put in 30 cm^3 Teflon-lined Morey-type autoclaves, inserted in steel chambers, and finally put in an oven at 190 ± 2 °C without stirring. The autoclaves were taken off the oven at predetermined times, cooled down in tap water. The pH of the samples was then measured, the solid products filtered and washed several times with distilled water until a neutral pH was obtained. The solid products were finally dried at ca. 100 °C for 24 h. The dried samples were crushed in an agath mortar in fine powder. The final crystalline phases were also treated by ultrasound in order to eliminate traces of remaining amorphous phases.

The nature of the solid and the degree of crystallinity were determined by X-ray powder diffraction using a Philips PW 1730/10 diffractometer, between 5° and 45° 2θ at a scanning speed of 0.02 s^{-1}.

The reference samples for quantitative measurement were obtained from the final crystalline products treated with ultrasounds in order to separate the well crystallized material from the remaining amorphous gel.

Thermal analyses (DSC, TG and DTG) of the crystalline products were made on a Netzsch STA 409 thermal analyzer scanning from 20 to 750 °C at a rate of 10 °C/min under a 15 ml/min nitrogen flow.

The size and shape of the crystallites were measured by SEM on a Stereo SCAN 360.

The NMR spectra were recorded on a Bruker MSL 400 spectrometer. For ^{29}Si (79.5 MHz) a 9.5 μs ($\theta = \pi/6$) pulse was used with a repetition time 4.0 s. For ^{13}C (100.6 MHz) a 5.0 μs ($\theta = \pi/2$) pulse, a single contact time and recycle time of 6.0 s were used. For ^{51}V (105.2 MHz) a 1.0 μs ($\theta = \pi/12$) pulse was used with a repetition time of 0.2 s.

3. Results and discussion

3.1. Crystal fields and crystallization rates

The crystallization fields obtained from gels of composition xNa$_2$O–yVO$_2$–7NaF–ySO$_3$–zSiO$_2$–2TPABr–260H$_2$O for $z = 12$ with $3.6 \leq x \leq 14.4$ and $2.1 \leq y \leq 7.1$, and for $x = 3.6$, $0.3 \leq y \leq 4.2$ and $4.0 \leq z \leq 12.0$ are shown in Fig. 1a and b.

It can be seen that the VO_2/Na_2O ratio influences the crystallization of V-MFI. Indeed, the necessary amount of VO_2 increases with increasing Na_2O content in the gel for constant SiO_2 (Fig. 1a). For example, the experimental points corresponding to $VO_2/Na_2O = 0.5$ are found in the crystallization fields of V-MFI zeolite. On the other hand, the ratio VO_2/SiO_2 does not influence, in a certain limit, the formation of V-MFI (Fig. 1b). In Fig. 1b, the 3.6 mol Na_2O are close to the 3.44 mol of Na_2O introduced by 12.0 mol of sodium silicate. For 3.6 mol of Na_2O, $z = 12.56$ represent the highest possible value in this system.

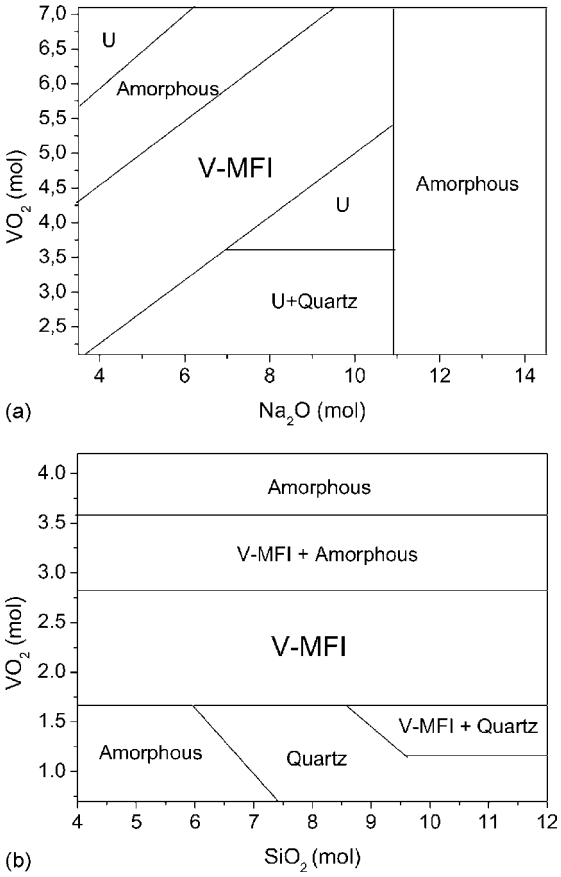

Fig. 1. Crystallization fields obtained from gels xNa$_2$O–yVO$_2$–7NaF–ySO$_3$–zSiO$_2$–2TPABr–260H$_2$O at 190 °C: (a) $z = 12.0$, $3.6 \leq x \leq 14.4$ and $2.1 \leq y \leq 5.6$; (b) $x = 3.6$, $0.7 \leq y \leq 4.2$ and $4.0 \leq z \leq 12.0$; U: unknown phase.

Fig. 2 represents the crystallization curves for the V-MFI zeolite. The crystallinity of the various samples were compared to the crystallinity of the most crystalline final sample separated from the remaining amorphous phase by sonication. Table 1 shows the induction time in hours (corresponding to the appearance of ca. 4% crystallinity) and the

Table 1
Induction time (in hours) and crystallization rate (in percentage per hour) for V-MFI zeolites obtained from gels xNa$_2$O–yVO$_2$–7NaF–ySO$_3$–zSiO$_2$–2TPABr–260H$_2$O at 190 °C

x	y	z	t_{ind} (h)	R (% h^{-1})
3.6	2.1	12.0	3.1	5.0
3.6	2.8	12.0	3.2	4.0
5.4	4.2	12.0	6.9	10.0
6.3	4.2	12.0	7.5	15.7
7.2	4.2	12.0	3.0	3.8
7.2	4.9	12.0	5.8	13.4
7.2	5.6	12.0	3.8	5.3
3.6	2.1	4.0	7.5	3.5
3.6	2.8	4.0	3.8	11.4

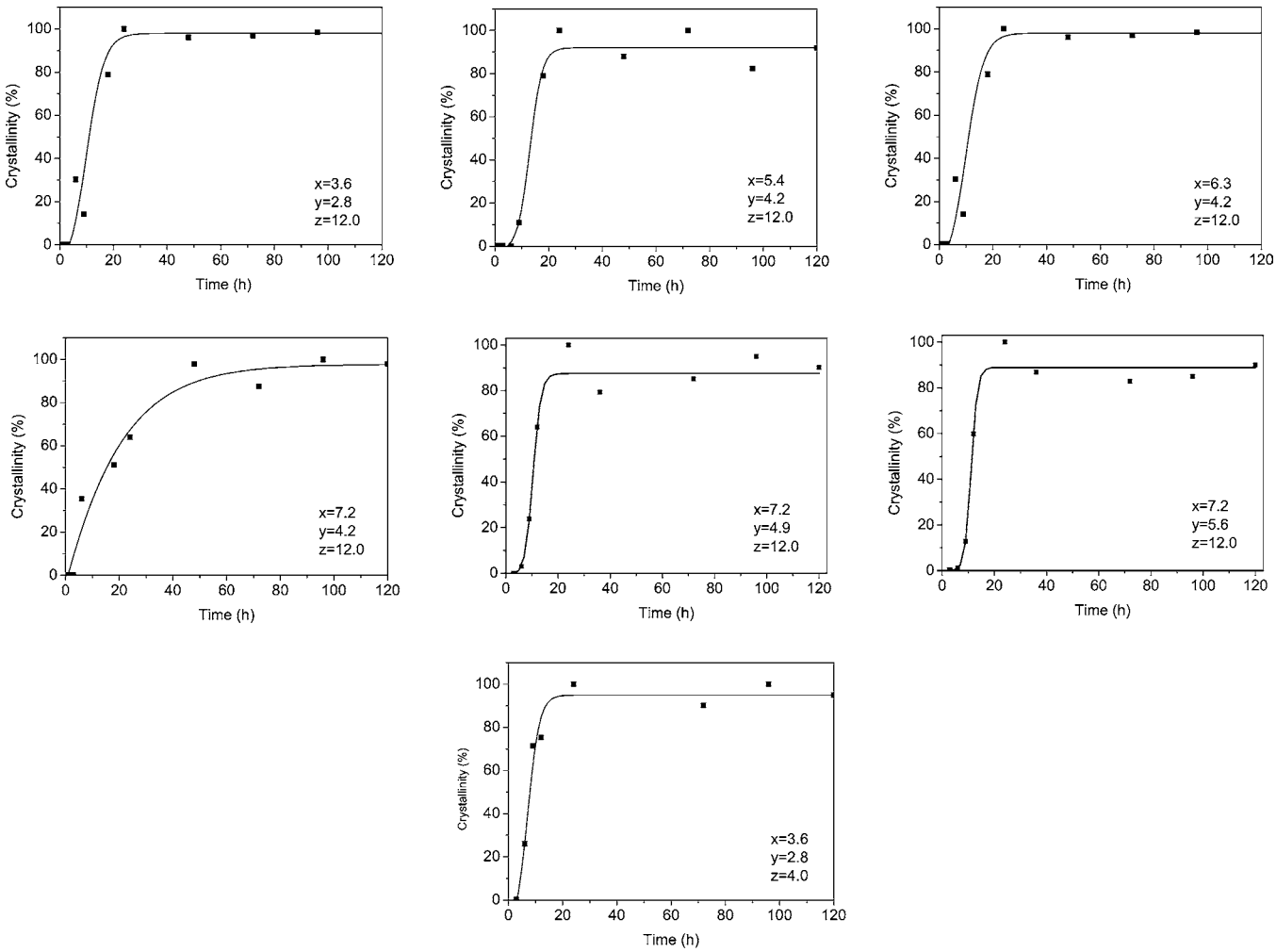

Fig. 2. Crystallization curves for the V-MFI zeolite at 190 °C from gels of composition xNa$_2$O–yVO$_2$–7NaF–ySO$_3$–zSiO$_2$–2TPABr–260H$_2$O.

crystallization rate (in percentage per hour), that is the maximum value of the crystallization curve's first derivatives.

For $x = 3.6$ and $z = 12.0$, the increase in V leads to a decrease of the crystallization rate, while the induction time remains constant. This suggests that the nucleation occurring also during the induction time is not modified, while the crystallization, i.e. the incorporation of V into the framework, is more difficult at higher V content. If the V and Si content of the gels remain constant ($y = 4.2$ and $z = 12.0$), the effect of alkalinity (increasing x values) is to increase first the induction time and the crystallization rate, but then both induction time and crystallization rate decrease again. This suggests that the alkalinity has an opposite effect on the nucleation rate and on the crystallization rate. It is thus not possible to arrive at present at clear-cut conclusions concerning the effect of alkalinity. At high alkalinity ($x = 7.2$) the effect of increasing V content has first an increasing effect on both induction time and crystallization rate, but at higher V content ($y = 5.6$) both the induction time and crystallization rate are decreasing again. Once again, it can be noticed that subtle effects are intervening in both the nucleation and reaction rates and our present results are not able to explain adequately all the phenomena that are occurring. Finally, only at low initial SiO$_2$ content ($z = 4.0$) are both the induction and crystallization rates increasing with increasing initial V content.

Table 2 shows the initial (pH$_i$) and final (pH$_f$) pH values for the synthesis of pure V-MFI phases. It can be seen that

Table 2
Initial (pH$_i$) and final (pH$_f$) pH values of the mother liquors during the synthesis of V-MFI zeolites from gels xNa$_2$O–yVO$_2$–7NaF–ySO$_3$–zSiO$_2$–2TPABr–260H$_2$O at 190 °C

$z = 12.0$				$x = 3.6$			
x	y	pH$_i$	pH$_f$	y	z	pH$_i$	pH$_f$
3.6	2.1	9.5	10.0	2.1	4.0	10.0	11.0
3.6	2.8	8.7	9.5	2.1	8.0	9.5	12.0
5.4	2.8	10.0	10.0	2.1	12.0	9.5	10.0
5.4	4.2	8.7	9.9	2.8	4.0	8.5	8.5
7.2	4.2	10.5	10.5	2.8	8.0	8.0	9.0
7.2	5.6	8.5	10.0	2.8	12.0	8.7	9.5

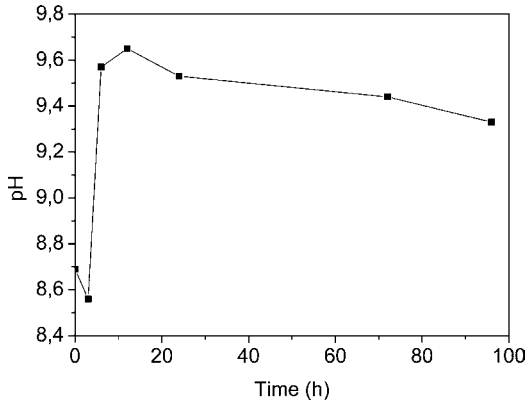

Fig. 3. Variation of pH as a function of time for the system $3.6Na_2O$–$2.8VO_2$–$7NaF$–$2.8SO_3$–$12.0SiO_2$–$2TPABr$–$260H_2O$.

in most of the cases the pH_f values are higher than the pH_i values, or they remain constant. It is particularly interesting to determine the variation of the pH during the crystallization [17,18]. Fig. 3 shows the variation of the pH values as a function of time for the system $3.6Na_2O$–$2.8VO_2$–$12SiO_2$. During the induction period (0–3 h), pH decreases due to the dissolution-depolymerization of the gel:

$$(RO)_3Si–O–Si(OR)_3 + OH^- \rightarrow (RO)_3Si–O^- + HOSi(OR)_3$$

with RO = OH, OSi or O^-. In the beginning of the crystallization, pH increases due to the condensation of silicate groups to form the zeolitic crystal:

$$(RO)_3Si–O^- + HOSi(OR)_3 \rightarrow (RO)_3Si–O–Si(OR)_3 + OH^-$$

When the dissolution of the solid phase of the gel and the formation of the crystals are reaching a steady state, pH is remaining quasi-constant.

The crystallization of V-MFI can also be followed by TG, DTG and DSC determination of the various intermediate and final phases [19]. Fig. 4 shows the DTG and DCS curves, while Table 3 gives the weight losses and the temperature of the maxima of the DSC curves. The total weight loss

Table 3
TG and DSC analysis of the intermediate and final V-MFI samples obtained from $3.6Na_2O$–$2.8VO_2$–$7NaF$–$2.8SO_3$–$12.0SiO_2$–$2TPABr$–$260H_2O$

t (h)	H_2O[a]		TPA[b]	
	T_{max}(DSC) (°C)	Weight loss (%)	T_{max}(DSC) (°C)	Weight loss (%)
6	145.4	8.2	440	3.8
12	93.8	5.6	457	9.6
24	88.9	2.9	445	10.9
72	214.7	0.1	436	11.4

[a] The weight loss is determined between 20 and 300 °C.
[b] The weight loss is determined between 300 and 700 °C.

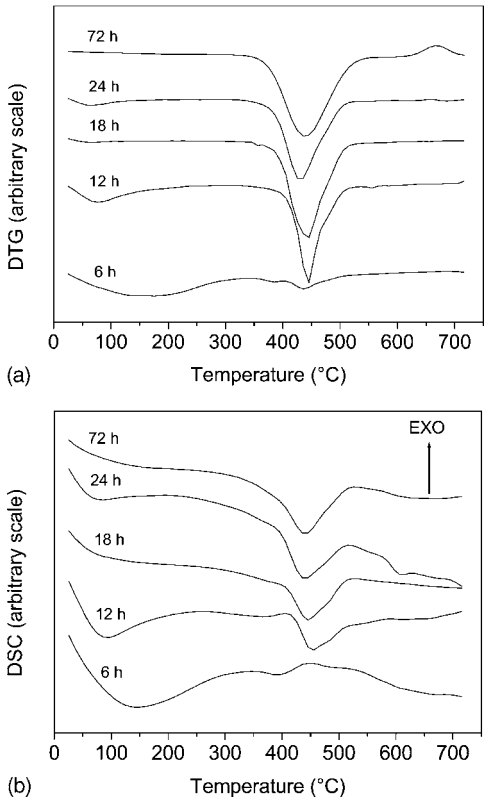

Fig. 4. DTG (a) and DSC (b) curves of intermediate and final V-MFI phases of system $3.6Na_2O$–$2.8VO_2$–$7NaF$–$2.8SO_3$–$12.0SiO_2$–$2TPABr$–$260H_2O$.

of H_2O is decreasing with increasing crystallization time, showing that the gel phase is more hydrophilic than the final crystalline V-MFI phase. On the other hand, the weight loss due to TPA present in the zeolitic channels increases with increasing crystallization time.

The observation of the crystals in the intermediate and final phases by SEM is most revealing. Indeed, it can lead to a precise picture on the relationship between the solid phase of the gel and the crystallites formed. Fig. 5 shows the SEM micrographs of the various intermediate and final samples obtained from $3.6Na_2O$–$2.8VO_2$–$7NaF$–$2.8SO_3$–$12SiO_2$–$2TPABr$–$260H_2O$ at 190 °C. At 3 h, the system is still in the amorphous phase. At 6 h, the first crystals start to appear and, which is an important observation, they are in contact with the solid phase of the gel. This suggests that both the nucleation and the crystallization steps take place at the interface of the solid phase of the gel and the liquid phase, as it was previously shown for the formation of MFI crystals in alkaline media [20]. The nutrients are transported through the liquid phase. At 12 h, some amorphous phase still remains in the sample, while at 18 h, pure twinned crystals also appear. After that time, the crystal sizes do not change much. The Si/V ratios determined by EDS and the size of the crystals together with the aspect ratios determined by SEM are reported in Table 4. The Si/V ratios are regularly increasing with increasing time, showing the

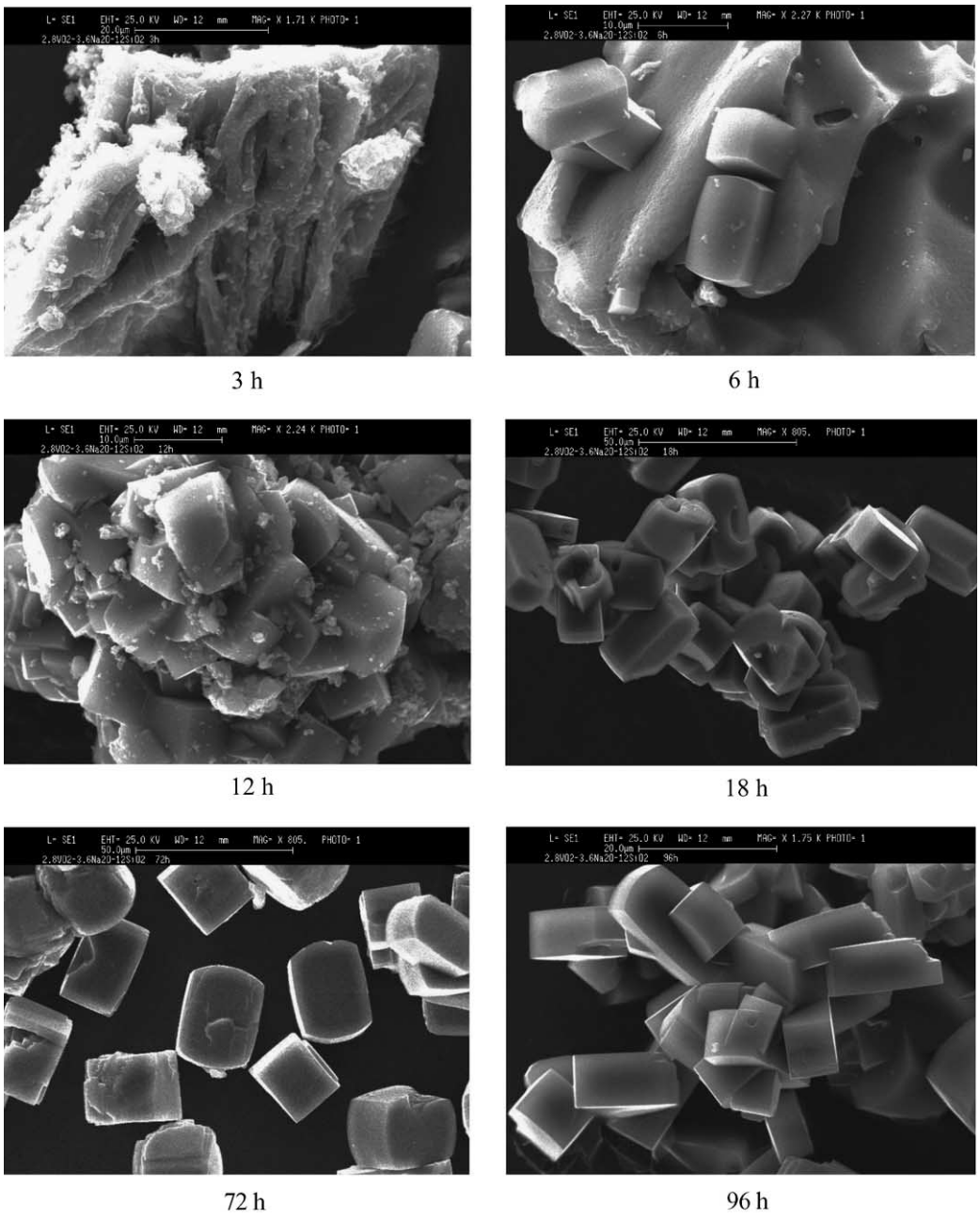

Fig. 5. SEM micrographs of the intermediate and final samples obtained from gel $3.6Na_2O$–$2.8VO_2$–7NaF–$2.8SO_3$–$12.0SiO_2$–2TPABr–$260H_2O$.

Table 4
Si/V ratios determined by EDS, dimensions (μm) and aspect ratios of the V-MFI crystals obtained from gels $3.6Na_2O$–$2.8VO_2$–7NaF–$2.8SO_3$–$12.0SiO_2$–2TPABr–$260H_2O$

t (h)	Si/V	*L* (μm)	*W* (μm)	*T* (μm)	*L*/*W*	*L*/*T*
3	4.8	Amorphous			–	–
6	12.1	11.5	6.7	5.5	1.7	2.1
12	30.8	12.5	9.0	9.0	1.4	1.4
18	40.3	28.8	18.6	13.7	1.6	2.1
24	46.5	35.7	30.9	14.9	1.2	2.4
72	51.6	32.5	23.8	18.9	1.4	1.7
96	69.8	35.4	25.5	15.0	1.4	2.4

L: length; *W*: width; *T*: thickness.

impoverishment in vanadium of the outer 1 μm layer of the crystals. Indeed, EDS essentially explores the external layer of ca. 1 μm layer of the material [21]. The impoverishment in V could stem from the progressive incorporation of V in the crystals, depleting at the same time the solid phase of the gel in V.

The length (*L*) of the crystals increases with increasing crystallization time (Fig. 6 and Table 4). It is also true for the width (*W*) and the thickness (*T*) (Table 4). Interestingly, the aspect ratios, i.e. *L*/*W* and *L*/*T*, do not change much, *L*/*W* is close to 1.4 and *L*/*T* to 2.1 showing a proportional increase of the crystals in all directions.

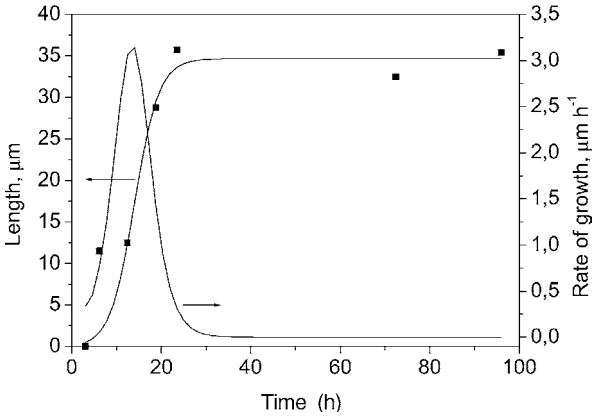

Fig. 6. Variation of length of the V-MFI crystals as a function of time for the samples obtained from gel $3.6Na_2O$–$2.8VO_2$–7NaF–$2.8SO_3$–$12.0SiO_2$–2TPABr–$260H_2O$.

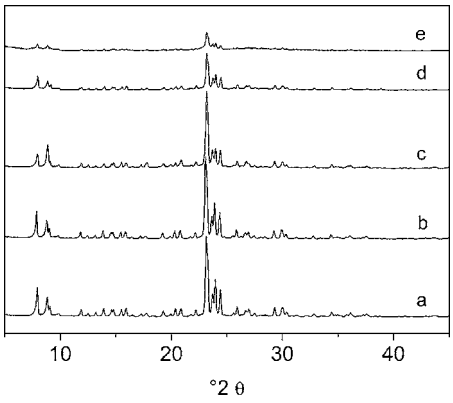

Fig. 7. XRD spectra of the samples obtained from: (a) $7.2Na_2O$–$5.6VO_2$–$12.0SiO_2$, V/u.c. = 1.1, pH_i = 8.5; (b) $3.6Na_2O$–$2.8VO_2$–$4.0SiO_2$, V/u.c. = 1.5; pH_i = 8.5; (c) $3.6Na_2O$–$2.5VO_2$–$4.0SiO_2$, V/u.c. = 2.4, pH_i = 8.5; (d) $3.6Na_2O$–$2.1VO_2$–$8.0SiO_2$, V/u.c. = 8.0, pH_i = 9.5; (e) $7.2Na_2O$–$4.2VO_2$–$12.0SiO_2$, V/u.c. = 10.6, pH_i = 10.5.

3.2. Characterization of the final V-MFI crystals

The chemical analysis of the various final V-MFI phases was carried out using atomic absorption. The data are reported in Table 5. It is interesting to note that Na^+ is accompanying V in the V-MFI zeolite. In most of the cases, for constant Na_2O and SiO_2 values, the V/u.c. values are decreasing with increasing V in the gel.

It is interesting to compare the Si/Na, V/Na and Si/V ratios in the gel and in the final V-MFI samples (Table 6). Generally a higher amount of V is introduced into the sample with respect to Na^+ ions. The introduction of V is very inefficient with respect to Si; this is due to the highly siliceous nature of all silicon MFI zeolite. Note that the initial pH values are close to 8.5 for all the well crystalline MFI samples. For higher initial pH values, less crystalline materials are obtained. This is also shown by the corresponding XRD spectra (Fig. 7). When the initial pH values are higher, much

Table 5
Chemical analysis of final V-MFI samples obtained from xNa_2O–yVO_2–7NaF–ySO_3–$zSiO_2$–2TPABr–$260H_2O$ at 190 °C

x	y	z	V/u.c.	Na/u.c.
3.6	2.8	4.0	1.5	1.2
3.6	3.5	4.0	2.4	1.2
3.6	2.8	8.0	3.5	3.6
3.6	1.4	12.0	4.1	4.5
3.6	2.8	12.0	1.8	1.4
5.4	4.2	12.0	1.3	0.3
7.2	5.6	12.0	1.1	0.6

Reaction time: 3 days.

Table 6
Si/V, Si/Na and V/Na ratios in the gel and in the final crystalline V-MFI samples obtained from xNa_2O–yVO_2–7NaF–ySO_3–$zSiO_2$–2TPABr–$260H_2O$ at 190 °C

x	y	z	$Si/V\|_{gel}$	$Si/Na\|_{gel}$	$V/Na\|_{gel}$	$V/Na\|_{u.c.}$	pH_i
3.6	2.8	4.0	1.43	0.56	0.39	1.25	8.5
3.6	2.8	8.0	2.86	1.11	0.39	0.99	8.0
3.6	2.8	12.0	4.29	1.67	0.39	1.31	8.7
5.4	4.2	12.0	2.86	1.11	0.39	4.40	8.7
7.2	5.6	12.0	2.14	0.83	0.39	1.83	8.5

Reaction time: 3 days.

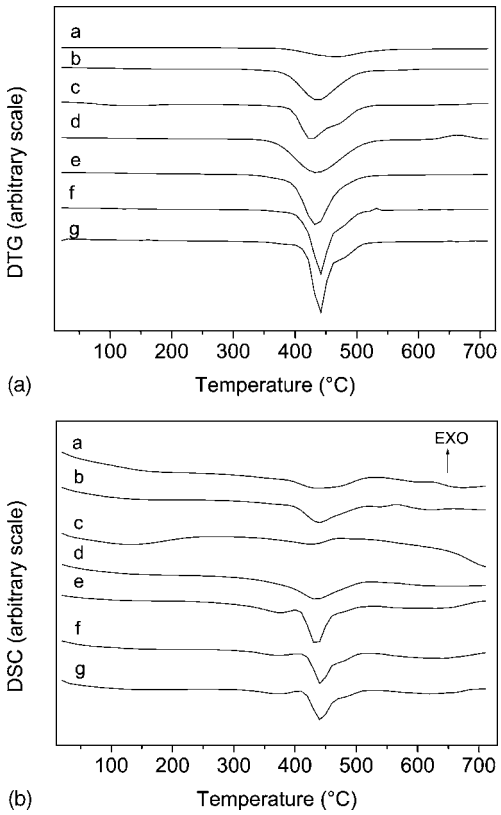

Fig. 8. DTG (a) and DSC (b) curves of samples obtained from (a) $3.6Na_2O$–$1.4VO_2$–$12.0SiO_2$, V/u.c. = 4.1, pH_i = 8.0; (b) $3.6Na_2O$–$2.8VO_2$–$8.0SiO_2$, V/u.c. = 3.5, pH_i = 8.0; (c) $3.6Na_2O$–$3.5VO_2$–$4.0SiO_2$, V/u.c. = 2.4, pH_i = 8.5; (d) $3.6Na_2O$–$2.8VO_2$–$12.0SiO_2$, V/u.c. = 1.8, pH_i = 8.7; (e) $3.6Na_2O$–$2.8VO_2$–$4.0SiO_2$, V/u.c. = 1.5, pH_i = 8.5; (f) $5.4Na_2O$–$4.2VO_2$–$12.0SiO_2$, V/u.c. = 1.3, pH_i = 8.7; (g) $7.2Na_2O$–$5.6VO_2$–$12.0SiO_2$, V/u.c. = 1.1, pH_i = 8.5.

Table 7
TG and DSC analysis of final crystalline V-MFI samples obtained from xNa$_2$O–yVO$_2$–7NaF–ySO$_3$–zSiO$_2$–2TPABr–260H$_2$O at 190 °C

x	y	z	V/u.c.	H_2O		TPA						TPA/u.c. total loss
				T_{max}(DSC) (°C)	H_2O/u.c. loss	Peak I		Peak II		Peak III		
						T_{max}(DSC) (°C)	TPA/u.c. loss	T_{max}(DSC) (°C)	TPA/u.c. loss	T_{max}(DSC) (°C)	TPA/u.c. loss	
3.6	2.8	12.0	1.8	171	0.3	372	0.7	435	2.0	476	0.9	3.6
5.4	4.2	12.0	1.3	183	0.9	378	0.4	447	2.4	478	1.0	3.8
7.2	5.6	12.0	1.1	159	0.8	374	0.4	441	2.3	472	1.1	3.8
3.6	1.4	12.0	4.1	188	3.3	383	0.1	429	0.4	475	1.1	1.6
3.6	2.8	4.0	1.5	147	0.6	379	0.5	437	2.6	474	0.9	4.0
3.6	2.8	8.0	3.5	160	0.4	383	0.3	445	1.9	472	0.9	3.1
3.6	3.5	4.0	2.4	124	2.8	368	0.3	425	1.8	484	1.3	3.4

Reaction time: 3 days.

less crystalline samples are obtained with a high V content where V is not incorporated in the structure.

The DTG curves and DCS curves of the final crystalline V-MFI samples are illustrated in Fig. 8a and b, respectively. Table 7 reports the weight losses and the temperature of the maxima of the DSC curves.

The small peak at ca. 375 °C was interpreted as due to TPA^+ ions extending at the external surface of the crystallites [27]. The second DSC peak at ca. 430 °C is due to the decomposition of the TPA^+ ions to form tripropylamine, dipropylamine, propylamine and propylene [28]. Finally, the third DSC peak at ca. 475 °C is due to the decomposition of the decomposition products stemming from the second peak [28].

Fig. 9 shows the high-power decoupled ^{13}C-NMR spectrum of TPA^+ ions occluded in the V-MFI channels. The chemical shifts are characteristic of silicalite-1 synthesized in fluoride-containing media [22,23] or in alkaline media [24]. This means that the small amounts of V in the samples do not influence significantly the ^{13}C-NMR spectra of occluded TPA^+ ions. It can be said that the interaction between the carbon atoms and the zeolitic wall is similar in both cases. Note the two different lines for the CH_3 groups stemming from the fact that two groups are in the linear channels and the other two groups are in the zig-zag channels.

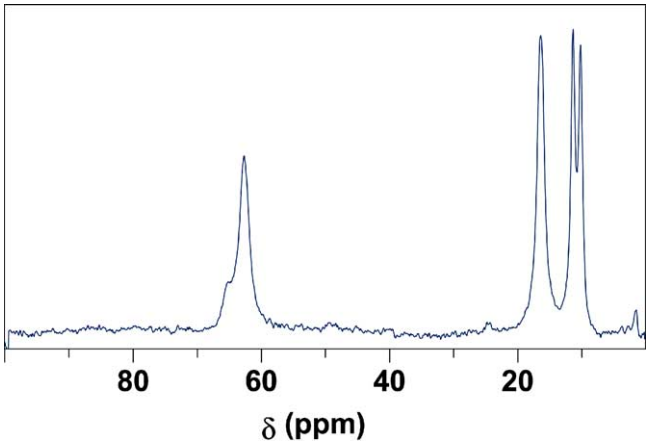

Fig. 9. Typical ^{13}C NMR spectrum of TPA occluded in final crystalline V-MFI sample obtained from 3.6Na$_2$O–3.5VO$_2$–7NaF–3.5SO$_3$–4.0SiO$_2$–2TPABr–260H$_2$O.

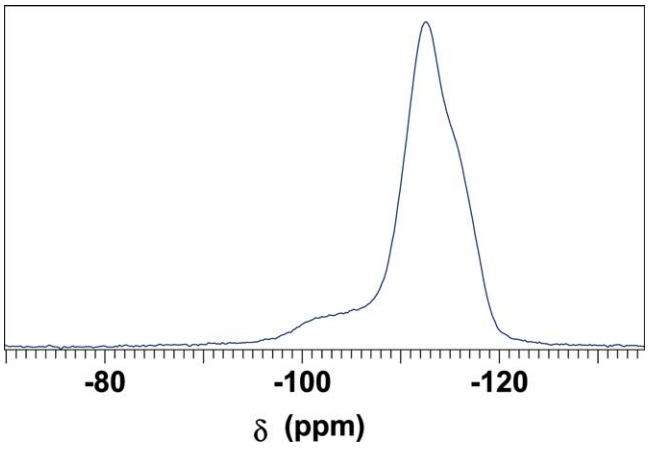

Fig. 10. Typical ^{29}Si NMR spectrum of final crystalline V-MFI sample obtained from 3.6Na$_2$O–2.8VO$_2$–7NaF–2.8SO$_3$–4.0SiO$_2$–2TPABr–260H$_2$O.

The ^{29}Si-NMR spectra of the V-MFI samples are characteristic of as-made silicalite-1. The spectrum is characteristic of an orthorhombic symmetry [24], it is composed of a shoulder at ca. −118 ppm, a maximum at −112.6 ppm, these lines stemming from Si(OSi)$_4$ configurations and of a line at −103 ppm stemming from ≡SiOH defect groups [24] (Fig. 10). Although the defect groups in silicalite-1 can account for up to 32/u.c., in these samples these values go only up to 48/u.c. and are on the average equal to 10% (Table 8). If one is supposing that the vanadium (IV) is incorporated into the framework as [2]

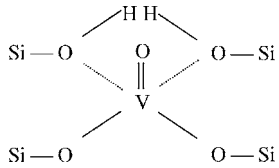

then two ≡SiOH groups are linked per 1 V/u.c. It can be seen that the amount of ca. 10/u.c. are more than enough to explain the introduction of V into the framework. Hence, some ≡SiOH defect groups stem also from the normal all siliceous MFI structure.

The ^{51}V-NMR spectra are more revealing. These spectra, although characterized by a chemical shift of −575 ppm versus $VOCl_3$ only stem from not well crystalline samples (see, e.g., spectra (d) and (e) in Fig. 7). In addition, all these spectra contain an additional ^{29}Si-NMR line at ca. −85 ppm. It is

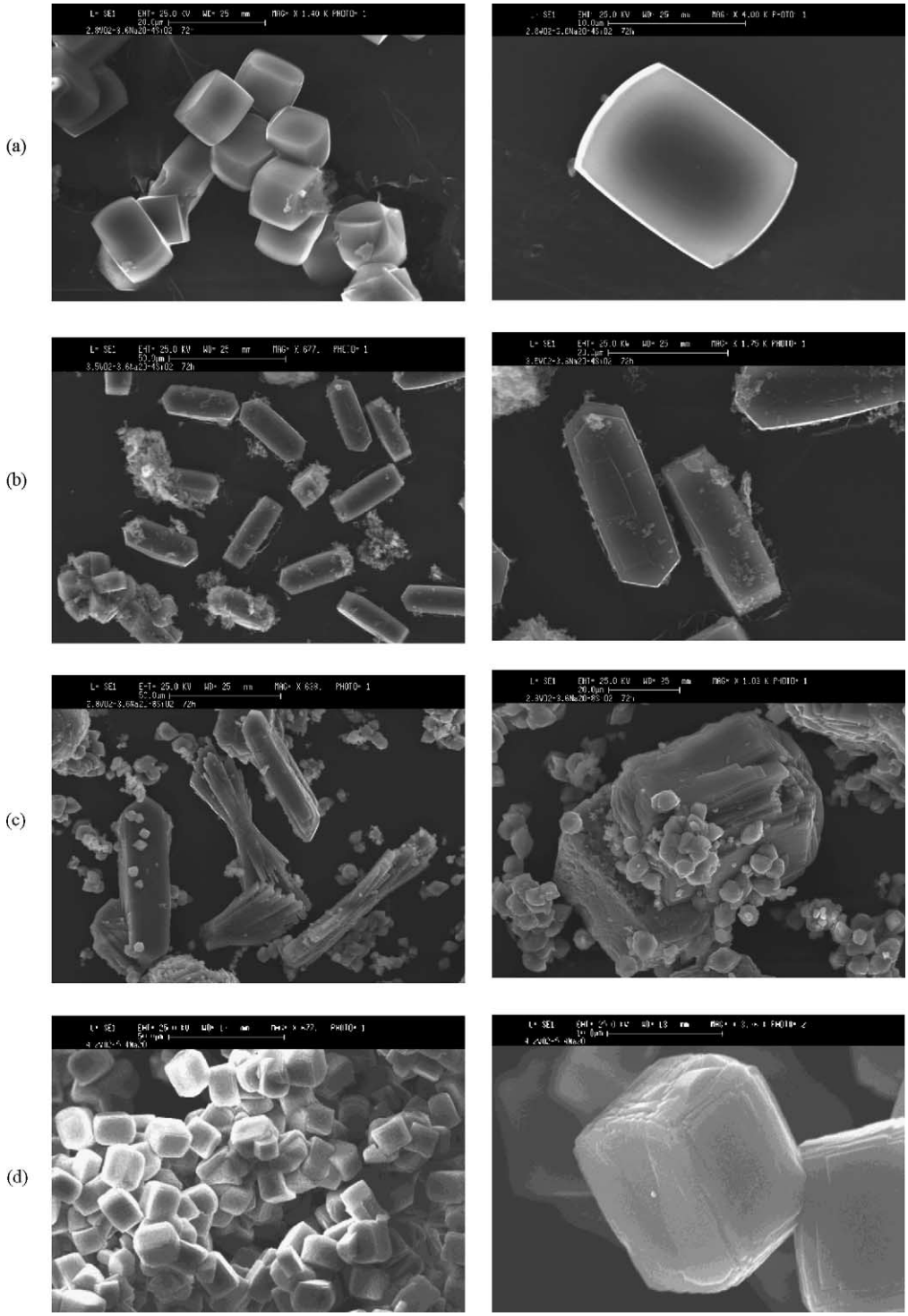

Fig. 11. SEM micrographs of final crystalline V-MFI phases obtained from xNa$_2$O–yVO$_2$–7NaF–ySO$_3$–zSiO$_2$–2TPABr–260H$_2$O at 190 °C with: (a) x = 3.6; y = 2.8; z = 4.0; (b) x = 3.6; y = 3.5; z = 4.0; (c) x = 3.6; y = 2.8; z = 8.0; (d) x = 5.4; y = 4.2; z = 12.0 (micrographs on the left and on the right have different scale).

Table 8
^{29}Si-NMR data of final crystalline V-MFI samples obtained from xNa$_2$O–yVO$_2$–7NaF–ySO$_3$–zSiO$_2$–2TPABr–260H$_2$O at 190 °C

x	y	z	V/u.c.	δ (ppm)	
				≡SiOH/u.c. (−103)	Si(OSi)$_4$/u.c. (−112.6)
3.6	2.8	12.0	1.8	10	86
5.4	4.2	12.0	1.3	9	87
7.2	5.6	12.0	1.1	10	86
3.6	1.4	12.0	4.1	(5)[a] 11	80
3.6	2.8	4.0	1.5	12	84
3.6	2.8	8.0	3.5	18	78
3.6	2.5	4.0	2.4	11	85

Reaction time: 3 days.
[a] Another line at −93 ppm is also detected due probably to a different phase or to more defects in the structure.

thus suggested that this V(V) species stem from an open not crystalline phase of silico-vanadium structure, where the V atoms have been oxidized already in the as-made samples. Indeed, for samples well characterized by all the physico-chemical techniques – XRD, thermal analysis, ^{29}Si-NMR (Table 8) – no ^{51}V-NMR spectra could be taken due to paramagnetic V(IV) species. These V(IV) species are only transformed into V(V) species during calcination [2]. It has to be emphasized that the presence of the ^{51}V-NMR line at −575 ppm in the as-made sample is not a definite proof that the V atoms occupy framework positions in the structure.

The SEM micrographs are illustrated in Fig. 11. The typical prismatic form can be recognized in all pictures. However, the size of crystals, their twinning, round corners, etc. are different from one sample to the other in these crystalline V-MFI materials. These crystals are rather big and can be compared to those obtained by Sand and coworkers [25,26]. Table 9 shows the crystal sizes and shapes together with the Si/V ratio determined by EDS for some samples. Although the length of the crystals varies between 15 and 41 μm, the aspect ratios, i.e. length/width, are close to 1.5 in most of the samples. This means that the rate of the crystal growth is similar in all conditions studied and it is not dependent on either the Na, or the V and Si contents. The Si/V values or the V/u.c. values can be compared with those obtained by atomic absorption (Table 5). As the penetration depth of the X-rays is ca. 1 μm [21], it can be concluded that the crystals obtained with 5.4Na$_2$O–4.2VO$_2$–12.0SiO$_2$ are quite homogeneous as the global composition (V/u.c. = 1.3) is quite close to that determined by EDS (V/u.c. = 1.2). On the other hand, the crystals obtained with 3.6Na$_2$O–2.8VO$_2$–12.0SiO$_2$ are less rich in V in the external 1 μm layer (V/u.c. = 1.0) than in the interior of the crystals (V/u.c. = 1.8).

Table 9
Morphology, size and Si/V ratios for final crystalline samples obtained from xNa$_2$O–yVO$_2$–7NaF–ySO$_3$–zSiO$_2$–2TPABr–260H$_2$O at 190 °C

x	y	z	Si/V[a]	L (μm)	W (μm)	L/W	Morphology
3.6	2.8	4.0		15.3	11.0	1.4	Rounded hexagonal prisms
3.6	3.5	4.0		33.0	11.1	3.0	Elongated hexagonal prism
3.6	2.8	8.0		34.0	23.1	1.5	Irregular shape
3.6	2.8	12.0	92.7	32.5	23.8	1.4	Rounded hexagonal prisms
5.4	4.2	12.0	78.0	41.0	31.8	1.3	Rounded hexagonal prisms
7.2	5.6	12.0		34.1	23.7	1.5	Rounded hexagonal prisms

Reaction time: 3 days.
[a] EDS values: V/u.c. = 1.0 and 1.2, respectively.

4. Conclusions

Up to about 4 V/u.c. can be easily introduced in the MFI structure using fluoride medium. The initial pH of the gels does not have to be higher than 9.0. The V atoms are incorporated as V(IV) in the structure, introducing two ≡SiOH defect groups at the same time:

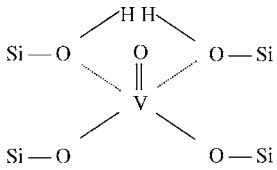

The TPA$^+$ ions are incorporated intact into the highly siliceous MFI structure.

Acknowledgements

The authors are indebted to Mr. Guy Daelen for taking the NMR spectra and for preparing the corresponding figures. The authors appreciate the help of Engineer Danilo Vuono for having produced the micrographs and the help of Mr. Michelangelo Bruno. The authors thank the Belgian Program on Inter University Piles of Attraction initiated by Belgian State, Prime Minister's Office for Scientific, Technical and Cultural Affairs (OSTC-PAI-IVAP No. P 5/01 on quantum size effects in nanostructured materials), and partly by Italian Research Council, Progetto Finalizzato Materiali 2.

References

[1] J.C. Védrine, Stud. Surf. Sci. Catal. 69 (1991) 25.
[2] A.M. Prakhash, L. Kevan, J. Phys. Chem. B 104 (2000) 6860.
[3] G. Bellussi, M.S. Rigutto, Stud. Surf. Sci. Catal. 85 (1994) 177.
[4] A. Miyamoto, D. Medhanavyn, T. Inui, Appl. Catal. 28 (1986) 89.
[5] A. Miyamoto, Y. Iwamoto, H. Matsuda, T. Inui, Stud. Surf. Sci. Catal. 49 (1989) 1233.
[6] K. Habersberger, P. Jiru, Z. Tvaruzkova, C. Centi, F. Trifiro, React. Kinet. Catal. Lett. 39 (1989) 95.
[7] L.W. Zatorki, G. Centi, J. Lopez Nieto, F. Trifiro, G. Bellussi, V. Fattore, Stud. Surf. Sci. Catal. 49 (1989) 1243.

[8] P.R. Hari Prasad Rao, R. Kumar, A.V. Ramaswamy, P. Ratnasamy, Zeolites 13 (1993) 663.
[9] P.R. Hari Prasad Rao, A.V. Ramaswamy, P. Ratnasamy, J. Catal. 137 (1992) 225.
[10] M.S. Rigutto, H. Van Bekkum, Appl. Catal. 68 (1991) L1.
[11] P. Fejes, J. Halàsz, I. Kiricsi, Z. Kele, I. Hannus, C. Fernandez, J. B.Nagy, A. Rockenbauer, Gy. Schöbel, in: L. Guczi, et al. (Eds.), New Frontiers in Catalysis: Part A, Akadémiai Kiadò, Budapest, 1993, p. 421.
[12] J.L. Guth, H. Kessler, M. Bourgogne, R. Wey, Brevet Fr. 2 564 451 (1985).
[13] F. Testa, R. Chiappetta, F. Crea, R. Aiello, A. Fonseca, J. B.Nagy, Colloids Surf. A 115 (1996) 223.
[14] F. Testa, F. Crea, R. Aiello, J. B.Nagy, Stud. Surf. Sci. Catal. 125 (1999) 165.
[15] E. Nigro, F. Crea, F. Testa, R. Aiello, P. Lentz, J. B.Nagy, Micropor. Mesopor. Mater. 30 (1999) 199.
[16] E. Nigro, F. Testa, R. Aiello, P. Lentz, A. Fonseca, A. Oszkò, P. Fejes, A. Kukovecz, I. Kiricsi, J. B.Nagy, Stud. Surf. Sci. Catal. 135 (2001) 04-P-18.
[17] J.L. Casci, B.M. Lowe, Zeolites 3 (1983) 186.
[18] K.R. Franklin, B.M. Lowe, Zeolites 8 (1988) 495.
[19] Z. Gabelica, J. B.Nagy, P. Bodart, A. Nastro, Thermochim. Acta 93 (1985) 749.
[20] J. B.Nagy, P. Bodart, H. Collette, Z. Gabelica, A. Nastro, R. Aiello, J. Chem. Soc. Faraday Trans. 1 85 (1989) 2749.
[21] G. Debras, A. Gourgue, J. B.Nagy, G. De Clippeleir, Zeolites 5 (1985) 369.
[22] J.M. Chézeau, L. Delmotte, J.L. Guth, M. Soulard, Zeolites 9 (1989) 78.
[23] A. Fonseca, J. B.Nagy, J. El Hage-Al Asswad, R. Mostowicz, F. Crea, F. Testa, Zeolites 15 (1995) 259.
[24] G. Engelhardt, D. Michel, High Resolution Solid-State NMR of Silicates and Zeolites, Wiley, Chichester, 1987.
[25] M. Ghammi, L.B. Sand, Zeolites 3 (1983) 155.
[26] R. Mostowicz, L.B. Sand, Zeolites 3 (1983) 221.
[27] J. B.Nagy, P. Bodart, H. Collette, J. El Hage-Al Asswad, Z. Gabelica, R. Aiello, A. Nastro, C. Pellegrino, Zeolites 8 (1988) 209.
[28] J. El Hage-Al Asswad, N. Dewaele, J. B.Nagy, R.A. Hubert, Z. Gabelica, F. Crea, R. Aiello, A. Nastro, Zeolites 8 (1988) 22.